Detecting Neural Currents Using Magnetic Resonance Imaging

An Honors Thesis (HONR 499)

by

Robin Klause

Thesis Advisor

Dr. Ranjith Wijesinghe

Ball State University

Muncie, IN

November 2018

Expected Date of Graduation

December 2018

Abstract

Current methods use blood oxygenation level-dependent contrast to indirectly detect neural activity but are inaccurate in their localization in space and time. Magnetic resonance imaging (MRI) has high space and time resolution, but it has not been shown to be feasible for detecting nerve signals. The action currents in nerves create their own magnetic field, which could potentially cause a large enough phase shift in the magnetic resonance signal to be detected. The possibility of direct imaging would benefit neuroscientists in their study of the human brain. In this thesis, COMSOL Multiphysics is used to simulate the displacement of ions in a copper sulfate solution as a model for the displacement of water molecules around nerves. If the water molecules experience a sufficient Lorentz force, their shift can be measured using MRI. The simulations do not conform to the results expected from articles on the same topic, due to errors and wrong assumptions in the model.

Acknowledgements

In the past three and a half years, I got to know many of the faculty and staff in the Department of Physics and Astronomy, all of whom have taught me valuable lessons, which I am very thankful for. They have all been great professors and have guided me through my experience as a physics major.

I wish to thank Mason Bole and Ben Simons who are former Ball State students and worked with Dr. Wijesinghe for teaching me the basics of the software I used for this research. Dr. Wijesinghe has not only been a great mentor throughout this project but has also supported me in other academic matters and I would like to thank him.

Contents

List of Figures

List of Equations

1 Author Statement

At the beginning of my sophomore year I was looking for scholarships and noticed that many of them required research experience, which I did not have at that time. I immediately wanted to get involved in a research project, not only because it was required by many scholarships, but also because I was interested in working on a real-world problem. I soon started to work in Dr. Wijesinghe's medical physics laboratory. Even though starting my first physics research project was exciting and interesting, it was also overwhelming, but I have learned important lessons during my time in the lab.

One of the challenges I was faced with when I started the project was that I had never learned about the physics concepts that were involved in the research. Being only a sophomore, I had not taken any advanced physics classes that covered magnetic moments, electromagnetic waves, or excitation states in enough detail to provide me with the necessary knowledge for the research. I had to learn and understand the concepts by myself, which has improved my ability to learn independently. I read textbooks and journal articles that often involved terminology I was not familiar with, but was able to understand after looking up more information. Because this interdisciplinary thesis relies on physics and biology, I not only had to learn about the physics of MRI, but also about the biology of nerves. The last biology class I took was in high school, so I had to refresh my memory on how nerve signals are transmitted in the brain.

Other valuable lessons came from learning how to use COMSOL Multiphysics, the software I worked with. The most obvious thing I learned was using the software itself, which can not only be used for this specific research, but also for many other simulations in completely different areas. While creating and testing my model, I experienced what many computer science instructors would tell their classes. When testing a program, it is important to change one part of the code at a time, or else you will not know what change caused the desired effect on the program. I often found myself changing multiple parameters at a time and I quickly lost track of what I had changed and what the outcome of that change was. After I had learned my lesson, I changed one part of the model at a time, so I could easily see what the effect was on my model.

One of the most exciting parts of this thesis was working on a real-life problem that is relevant in the world of medical physics. Usually the problems that are done in the class or in homework assignments have been solved before and have a definite solution. This problem, however, has not been solved before using the methods discussed in this thesis, and it is not even certain that there is a solution at all.

2 Introduction

The research in this thesis applies physics to the biological function of neural activity. Therefore, it is critical to not only discuss concepts of physics, which are mainly used in the research, but also concepts of biology to get the full spectrum of this work. First, in section 3, I introduce the structure of a nerve and the process of electrical and chemical nerve signals. Secondly, I explain concepts and equations that are necessary to understand the topic of this thesis and that are important in my research work. Section 5 gives an introduction to magnetic resonance imaging including some of the components necessary to form an image. This section also applies the physics concepts discussed in section 4 to MRI scanners. In section 6, I discuss the work that has already been done on this topic by other researchers. I review previous journal articles that form a basis of knowledge for this thesis. Finally, in sections 7 and 8, I show my results and provide a discussion on my findings, as well as a look into the future, proposing additional work that can be done based on this thesis.

3 Introduction to the Biology of Nerves

Almost all living organisms' ability to survive depends on how well they receive, process, and respond to information from the world around them and from their own cells. This ability depends on the effectiveness of communication between cells through networks of nerve cells, also called neurons. The exchange of information is accomplished through the transmission of electrical and chemical signals, called neural signals [20].

A neuron is composed of many parts. The cell body is the largest part of the neuron and contains the nucleus, the cytoplasm, and organelles. Dendrites extend from the cell body and receive stimuli and send signals to the cell body. The axon is also attached to the cell body and is responsible for sending electrical pulses to other neurons. The axon terminals release chemicals in the form of neurotransmitters that are used to communicate with other cells [20]. Figure 3.1 shows the composition of a neuron.

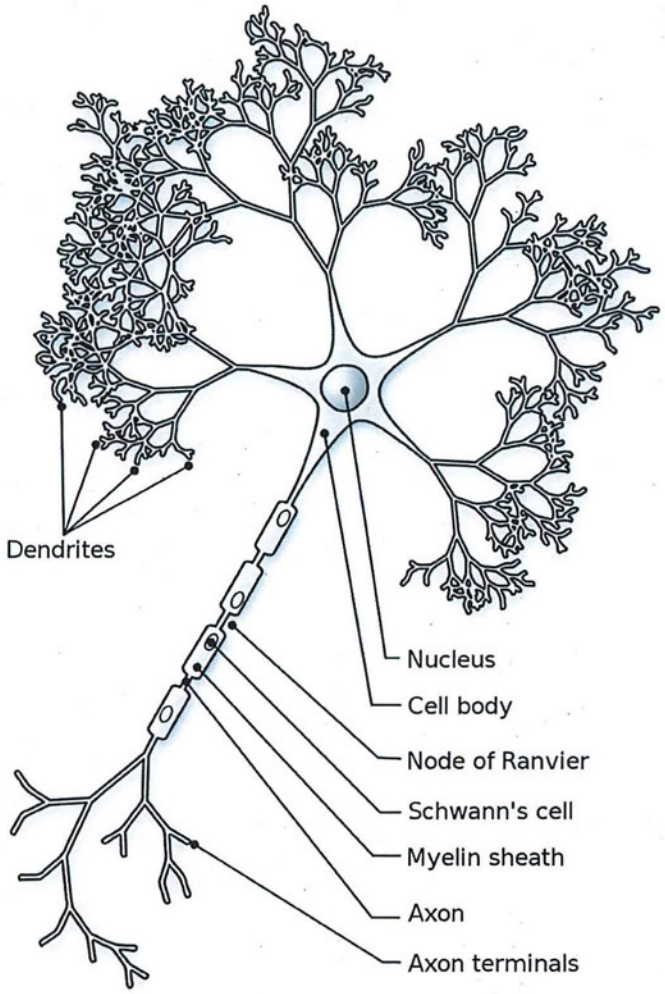

Figure 3.1: Composition of a neuron. From https://commons.wikimedia.org/wiki/File:Neuron-figure.svg. Used under the GNU Free Documentation License.

An inactive neuron has a resting potential of about -70 mV. This potential is caused mainly by potassium ions to diffuse out of the cell through passive ion channels. Sodium-potassium pumps also actively transport sodium out of the cell and potassium into the cell, but unequally. When three sodium ions are pumped out of the cell, only two potassium ions are pumped into the cell. Both of these processes cause a net positive charge on the outside of the cell, leading to a potential difference across the cell membrane.

When a stimulus is received and the voltage reaches a threshold level, sodium ion gates open and sodium ions flow into the cell. This decreases the negative charge on the inside of the cell and causes the negative potential to become positive. The so-called action potentials travels down the axon with a velocity between 0.6 and 100 meters per second [13]. After some time (~1 ms), the sodium channels close and the cell returns to its resting potential.

In contrast to electrical signals, chemical signals are sent with neurotransmitters across synapses, or junctions between two neurons or a neuron and another cell. There are many types of neurotransmitter, such as glycine, which transmits information in the brain and spinal cord. Neurotransmitters are stored in synaptic terminals and when an action potential reaches them, calcium ions cause the synaptic membrane to release neurotransmitters. These then travel across the synaptic gap, attach to receptors, and cause ion channels to open or close, which changes the potential and can set off an action potential [20].

4 Introduction to Physics

One force we experience at all times during our life is the gravitational force between us and the earth. This force is described by Newton's universal law of gravitation given by

$$F_G = G\frac{m_1 m_2}{r^2}, \tag{4.1}$$

where G is the universal gravitational constant, m_1 and m_2 are masses of objects 1 and 2 respectively, and r is the distance between the object [19]. This equation shows that the strength of the gravitational force is proportionally to the mass of the two objects and inversely proportional to the distance between the objects. More massive objects attract each other with a greater force, and objects that are further apart experience less force.

Mathematically similar, but different in nature is the Coulomb force that describes the force between two electrically charged objects and is given by

$$F_C = k_e\frac{q_1 q_2}{r^2}, \tag{4.2}$$

where k_e is Coulomb's constant, q_1 and q_2 are the charges of objects 1 and 2 respectively, and r is the distance between the objects [11]. While the mass of an object is always positive, the charge can be positive, negative, or zero. Therefore, the gravitational force is always positive, and thus attractive, while the electric force can be negative or positive, thus attractive or repulsive. If two objects have the same charge, making the force positive, they repulse, and if they have opposite charges, making the force negative, they attract.

Another key difference between gravitational and electric force is the magnitude or strength of the force determined by the constants G and k_e, the values of which are $G = 6.67 \times 10^{-11} Nm^2kg^{-2}$ and $k_e = 9.00 \times 10^9 Nm^2C^{-2}$. The gravitational force is about 40 orders of magnitude smaller than the electric force and is ignored in this thesis [12].

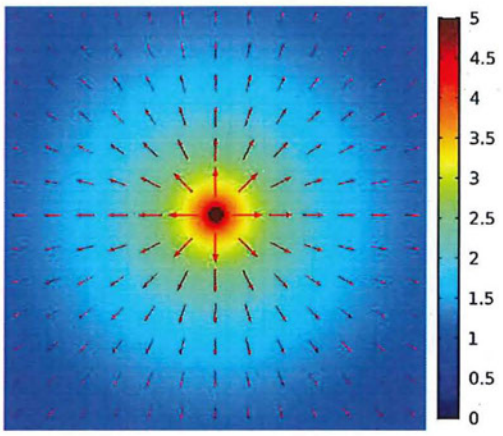

Figure 4.1: Electric field of a positive point charge at the center of the figure. The electric field is directed outward and its magnitude decreases as the distance from the charge increases. The color legend has arbitrary values.

Physicists often speak of gravitational or electric fields, rather than forces. A field only considers one object with mass or charge and describes its capability to exert a force on another object. Figure 4.1 above shows the electric field created by a positively charged object. The field is larger at closer distance to the charge, and with increasing distance, the field becomes weaker. The arrows on the field lines point away from the object, so a positive test charge (i.e., a one-dimensional point charge with one unit of charge) would feel pushed away from the object. A negative point charge would attract a positive test charge, so the arrows would point toward the location of the negative charge, but their magnitude would be the same.

Coulomb's force equation is limited by its ability to only describe the force between two stationary charges. Moving charges have different properties and create another type of field: the magnetic field. Conventionally, magnets are known to create a magnetic field, but moving charges do, too. Jean-Baptiste Biot and Félix Savart discovered a law that describes the magnetic field created by an electric current, which is composed of moving charges. The Biot-Savart law is given by

$$\vec{B} = \frac{\mu_0}{4\pi} \int \frac{I\, d\vec{l} \times \hat{r}}{r^2}, \tag{4.3}$$

where μ_0 is the permeability of free space, I is the current, $d\vec{l}$ is a differential length, and r is the position in space [11]. To understand the reason why moving charges create a magnetic field is difficult and requires knowledge of special relativity so it will not be discussed here (Purcell's Electricity and Magnetism). The magnetic field created by an infinitely long wire is shown in figure 4.2 below. The right-hand rule can be used to determine the direction of the field lines. Pointing the thumb in the direction of the current and curling the fingers around the thumb yields the direction of the magnetic field. By convention, the direction of the current is given by the direction of motion of positive particles, so when considering negative particles, the current direction is opposite to the direction of motion [19].

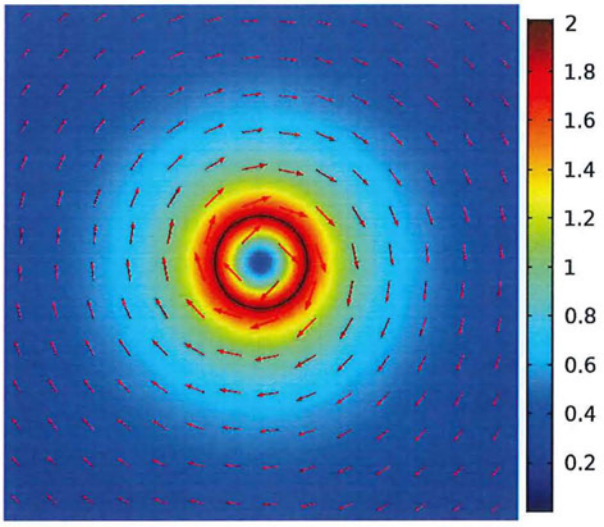

Figure 4.2: Magnetic field created by a current carrying wire. The current flows into the page, so according to the right-hand rule the magnetic field is in the clockwise direction. The magnetic field decreases as the distance from the wire increases. The color legend has arbitrary values.

As a consequence of the above forces and fields arises a new question. What is the behavior of moving objects in electric and magnetic fields? The Lorentz force combines the effects of the electric and magnetic forces on a point charge due to electromagnetic fields. The equation is given by

$$\vec{F} = q(\vec{E} + \vec{v} \times \vec{B}), \tag{4.4}$$

where q is the charge of the point charge moving with velocity $\vec{v}$ through an electric field $\vec{E}$ and a magnetic field $\vec{B}$ [11]. The part of the force that is due to the electric field ($q\vec{E}$) points in the same direction as the electric field itself. However, the part of the force that is due to the magnetic field ($q\vec{v} \times \vec{B}$) is perpendicular to both $\vec{v}$ and $\vec{B}$ due to the cross product between the two vectors. Another form of the right-hand rule can be used to determine the direction. When pointing the fingers of the right hand in the direction of $\vec{v}$ and turning the palm toward $\vec{B}$, the thumb will point in the direction of the force $\vec{F}$.

The Lorentz force equation can be applied to a current carrying wire, which confines charged particles within its boundaries. When individual moving particles experience a force they are deflected in the direction of the force, but since the wire forms a boundary for the particles, they will "bump" into the walls of the wire and cause the wire to experience a force. This force is given by

$$\vec{F} = I\vec{L} \times \vec{B}, \tag{4.5}$$

where I is the current in the wire, $\vec{L}$ is the length of the wire, and $\vec{B}$ is the magnetic field [11].

5 Magnetic Resonance Imaging

One of the key components of an MRI machine is a static magnetic field. The most obvious way to create a magnetic field is to use permanent magnets. However, these magnets have a fairly low magnetic field and are composed of rare-earth materials, which are expensive [6]. Additionally, permanent magnets cannot be turned on and off or controlled. A better solution is to use electrical currents. As described in the previous chapter, a current carrying wire creates a magnetic field, which is commonly called Ørsted field (named after Hans Ørsted who discovered this effect). A current carrying wire itself does not suffice for MRI because the field strength drops off as 1/r - which can be calculated using the Biot-Savart law - so the further the distance from the wire, the smaller the magnetic field [11]. What is instead used in current MRI technology are tightly wound coils of wires, called solenoids.

Solenoids produce a nearly uniform static magnetic field at their center of curvature as shown in figure 5.1. Mathematically, the magnetic field strength can be derived from the Biot-Savart law as follows

$$B = \mu_0 n I. \tag{5.1}$$

Here μ_0 is the permeability of free space, n is the number of turns per unit length, and I is the current through the solenoid [11]. The field is not only independent of any distances, as long as the position is in the center of the solenoid, but it can also be controlled. Increasing the current increases the magnetic field and turning the current off completely causes the magnetic field to turn off. Generally, MRI machines have magnetic field of 1.5 T, which is about 10,000 times stronger than the earth's magnetic field [26].

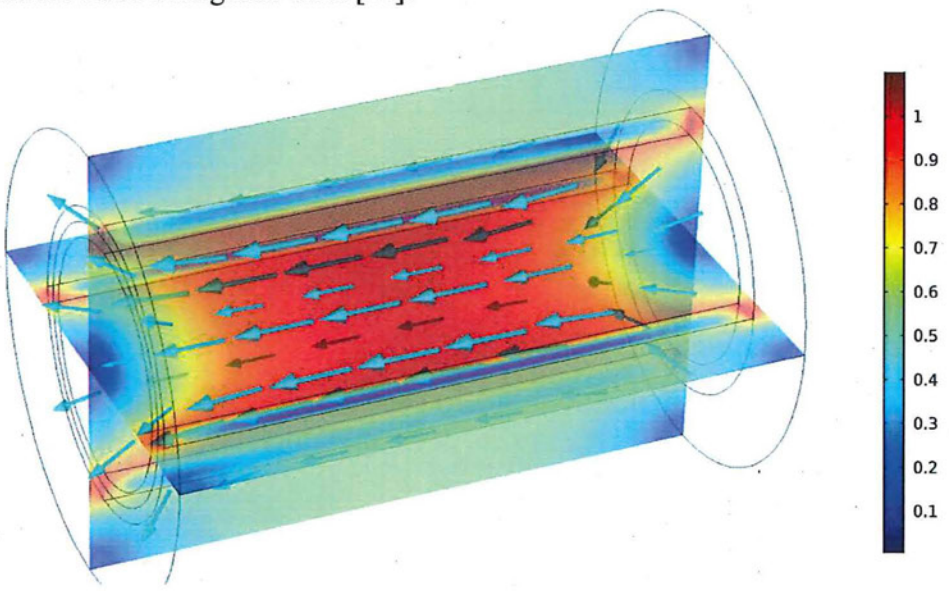

Figure 5.1: Magnetic field created by a solenoid. Arrows indicate the field direction. The color legend has arbitrary values.

All matter is composed of atoms, which contain protons, neutrons, and electrons. The most abundant and simple atom in the human body is hydrogen, which is contained in water molecules and is imaged in MRI. The single proton in the hydrogen atom has intrinsic spin, which can be thought of as the proton spinning about its central axis, similar to the earth spinning around its axis. The proton is positively charged, so its spin generates moving charges, which create a magnetic field, called magnetic moment. Another quantity that is created from the spin is angular momentum. Any object that rotates about an axis possesses angular momentum [34]. Using the right-hand rule, the direction of both magnetic moment and angular momentum can be determined to be along the axis of rotation, pointing up when the spin is counterclockwise, and down when the spin is clockwise.

Without an applied magnetic field, the proton spins are oriented randomly, but when placed in a uniform magnetic field their magnetic moment and therefore their axis of rotation line up parallel or antiparallel to the magnetic field. The parallel states have a lower energy than the antiparallel states. However, the axis of rotation is never perfectly lined up with the magnetic field, but rather moves about the magnetic field direction as shown in figure 5.2. This motion is called precession and is exhibited by all spinning object, such as gyroscopes or the earth.

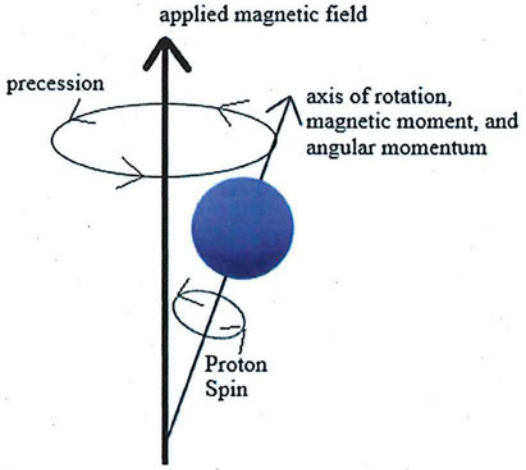

Figure 5.2: Precession of a proton spinning in the counterclockwise direction and having magnetic moment and angular momentum directed along the axis of rotation.

The precession of a proton occurs at a specific frequency called Larmor frequency, given by

$$\omega = \gamma B_0, \tag{5.2}$$

where B_0 is the magnetic field strength and γ is the gyromagnetic ratio of the proton, which is the ratio between the charge and mass of a proton [14, 26]. The Larmor frequency determines the frequency of electromagnetic radiation needed to excite spins to a higher energy [14].

The second word in magnetic resonance imaging suggests another important property needed to create and MR signal. Resonance is a phenomenon where oscillating objects or systems absorb energy at a specific resonant frequency. On a swing, for example, one has to move one's legs back and forth at the right time to increase the height of the swing. Moving the legs at the wrong time does not increase height and may even dampen the swing. Adding energy

to protons that are lined up in a magnetic field flips their magnetic moment direction from being parallel (lower energy) to being antiparallel (higher energy) with respect to the applied field. The supply of energy comes from an oscillating magnetic field in the form of an RF signal. RF stands for radio frequency and refers to the oscillation frequency of an electromagnetic waves. This frequency ranges from 20 kHz to 300 GHz, which means that the magnetic field oscillates 20,000 to 300 billion times in one second [8]. For a typical 1.5 T MRI scanner the resonant frequency is about 63.9 MHz (63.9 million times in one second) [26]. To generate the RF pulse, Radiofrequency coils are used. An alternating current with the resonant frequency is sent through a coil of wires and produces an alternating magnetic field at the same frequency. The equation for finding this frequency is identical to equation 5.2, so the Larmor and resonant frequencies are the same.

To obtain an MR signal, a short RF pulse is applied to the hydrogen nuclei contained in the water of the body, which causes the magnetic moments to align in the higher energy antiparallel state. When the RF pulse is stopped, the high-energy protons return to their thermodynamically favorable low-energy state (parallel to magnetic field). During this transition, protons lose energy in the form of emitted electromagnetic waves, which produce electric effects as described by Faraday's law: a changing magnetic field induces a voltage in a coil [11]. Different tissues in the body have different spin relaxation times, so the emitted signal differs for differing tissue and the voltage in the receiving coils changes. The induced voltage can be analyzed by computers to form an image. An example of an MRI image is shown in figure 5.3.

To get special resolution in the image, a gradient, or non-uniform magnetic field is applied instead of a uniform field as is mentioned at the beginning of this section. This makes the Larmor frequency slightly different at different locations, so specific parts of the body can be imaged.

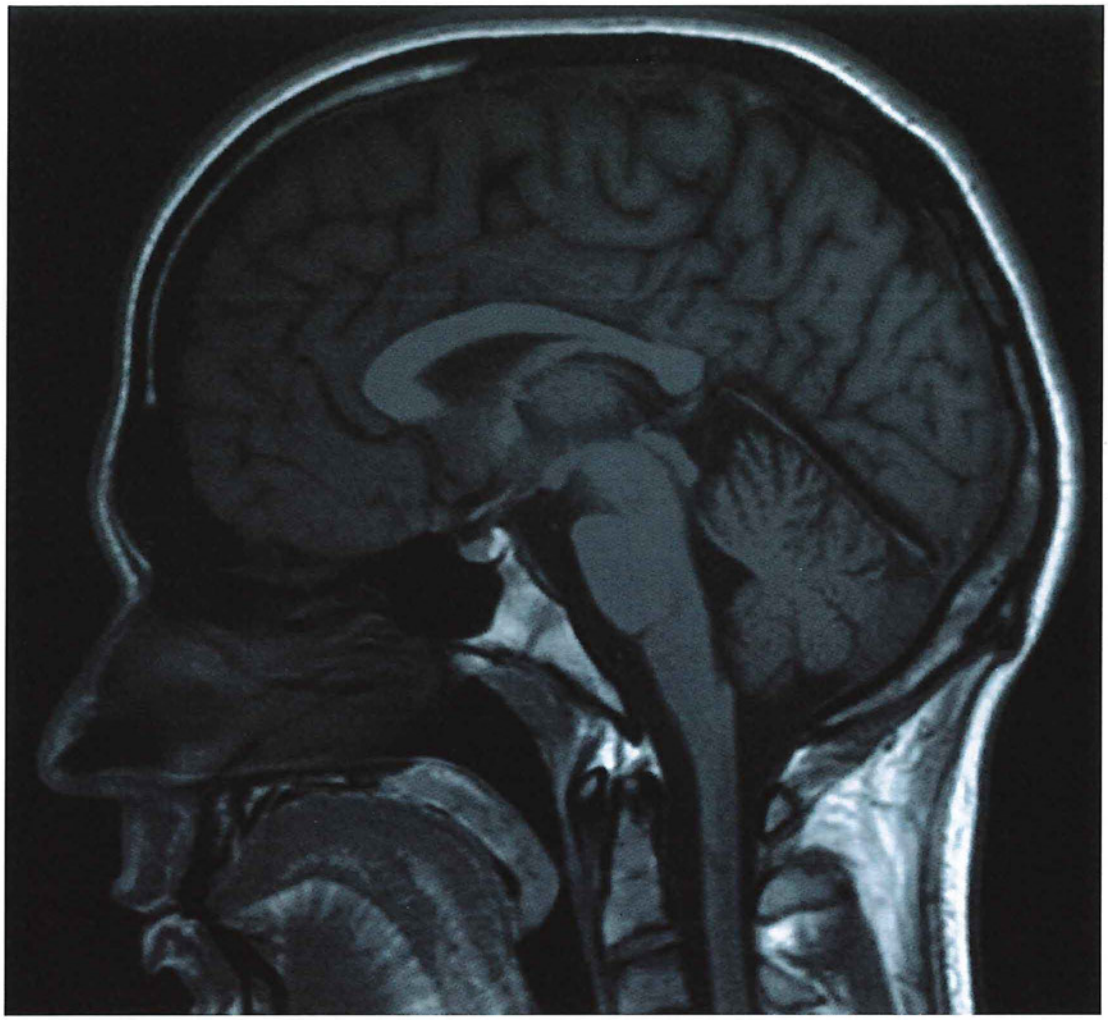

Figure 5.3: An image of a human head produced using MRI. From https://commons.wikimedia.org/wiki/File:Mrt_big.jpg. Used under the Creative Commons Attribution Share Alike 3.0 Unported License.

6 Detection of Neural Activity

The current technology for indirectly measuring neuronal activity is blood-oxygenation-level-dependent (BOLD) contrast. Here, metabolic consequences of nerve signals are measured, rather than the signals themselves. In order to maintain and restore neural potentials, energy in the form of glucose and oxygen is transported through the blood to active neurons. However, this technique has two major limitations: its spatial and its temporal resolution. Blood flows to active nerves from all directions even though neuronal activity occurs in precise locations, so it is not possible to precisely localize activity. There is also a time delay between neuronal activity and blood flow, which limits temporal resolution [14].

To improve the measurement of neural activity, many researchers have attempted to directly measure neural activity using different methods. Some have used numerical calculations [6, 22, 32], other have done experimental work using ferrite-core, wire wound toroids [5, 6, 9, 10, 18, 27, 29-31], or other experimental techniques [2-4, 16]. Although some of these report positive results [3, 17, 33], the direct detectability of nerve signals remains controversial [1, 15, 33]. The following research is preliminary work to this thesis, so it will be discussed in more detail.

Song and Takahashi introduced a technique for detecting minute electrical activity in a strong magnetic field called Lorentz effect imaging (LEI) [21]. As the name suggests, this method makes use of the Lorentz force shown in equation 4.4 and applied to a wire in equation 4.5. When a current carrying wire is subject to a magnetic field, it experiences a force perpendicular to the field. When the wire is placed in elastic material, it induces a spatially incoherent displacement of the material around it. Under a magnetic field gradient, the spins in the displaced region experience a change in magnetic moment direction and during the transition to the lower energy state, the signal is changed and can be picked up by an MRI scanner.

In their first experiment, Song and Takahashi enclosed a 1.5 mm copper wire with a cylindrical gel phantom that had similar elasticity to the brain and placed this structure into a constant magnetic field of 7 T. The Lorentz force causes a small displacement of the elastic material around it, which results in a detectable signal change. However, the currents of 200 μA and 500 μA that showed a detectable change in the image were several times larger than naturally occurring currents of nerve signals, so while their imaging method worked, their experiment was unrealistic. In a similar experiment, together with Truong, they optimized parameters and were able to detect 5 μA currents subject to a magnetic field of 4 T, which is more realistic [25].

Truong and Song then applied their LEI technique to the human median nerve and were able to image neuroelectric activity in vivo [24]. The next experiment servers as one of the basis for this thesis work [23]. Truong, Avram, and Song applied their technique to ionic currents in solutions to better characterize LEI. A spherical phantom with a $CoSO_4$ solution and two electrodes placed on opposite sides of the sphere was simulated. The ion trajectories could then be observed under the influence of the electric field created by the electrodes, and the magnetic field of the MRI scanner. The result of interest for this thesis is depicted in figure 6.1. The

positively charged copper ions moved away from the electrode with positive voltage and their trajectory was bent under the magnetic field. The negatively charged sulfate ions moved in the opposite direction toward the electrode with positive voltage and their trajectory was also bent under the magnetic field.

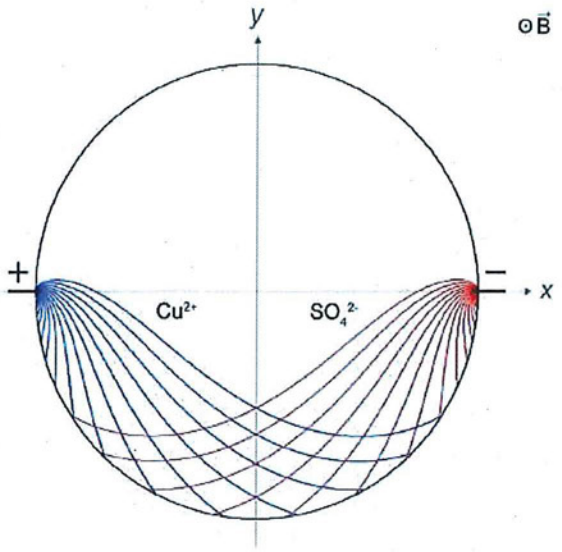

Figure 6.1: Simulated trajectories of a series of Cu^{2-} and SO_4^{2-} ions in a sphere containing a $CuSO_4$ solution exposed to a uniform static magnetic field and a dipolar electric field induced by two electrodes located on each side of the sphere. From [23]

Ion trajectories serve as a better model for nerve signals than electrical currents through a wire, since nerve signal transport occurs with ions as discussed in section 3. Since ions are electrically charged, their movement through a nerve creates a small current, which results in a magnetic field around the nerve as explained in section 4. The displacement of ions could cause a large enough change in proton spins to be detected with an MRI scanner. The abundance of water in the human body creates a good source of protons in the form of hydrogen atom nucleons. Directly measuring neural activity would allow scientists to use all the advantages of magnetic resonance imaging. They could non-invasively image nerve signals with high spatial and temporal resolution. This would allow doctors to better study brain diseases, such as Huntington's disease, Parkinson's disease, or Alzheimer's disease.

7 Model Simulation and Results

The simulations for this thesis were done on a desktop PC in the Medical Physics laboratory in the Cooper Science Building. The software used was COMSOL Multiphysics, which allows for three-dimensional model building and simulation.

The first task was to build a model as described in [23]. The geometry of this model consists of a sphere with a diameter of 10 cm, and two 5 mm long cylinders with a diameter of 4 mm inserted at either side of the sphere as depicted in figure 7.1. A cylindrical shape with a slightly larger diameter was cut out of the sphere to create a boundary between the inserted cylinders and the sphere. This is shown in figure 7.2. The sphere was filled with a 2.8 g/l $CuSO_4$ solution whose electrical conductivity was 1.4 S/cm. The two inserted cylinders served as electrodes and were made of copper.

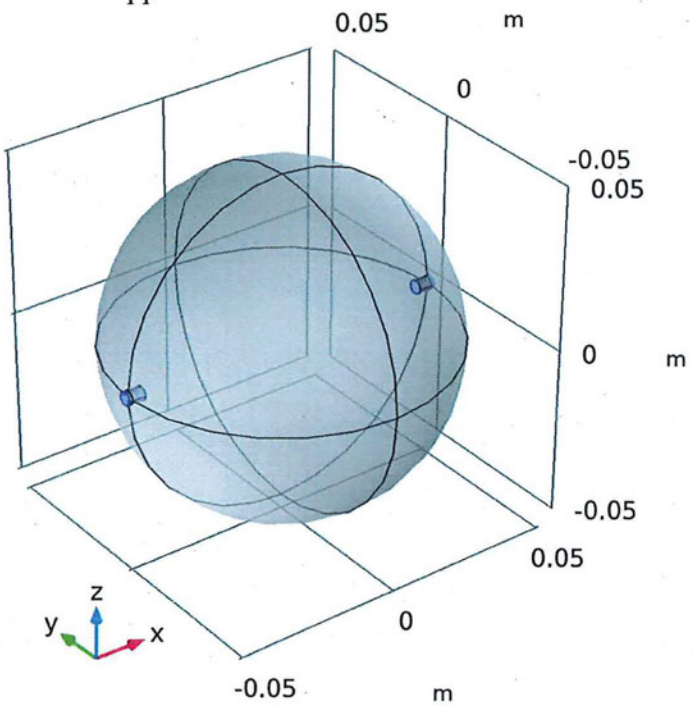

Figure 7.1: Model of a sphere with diameter of 10 cm and two 5 mm long cylinders with a diameter of 4 mm inserted at opposite sides of the sphere.

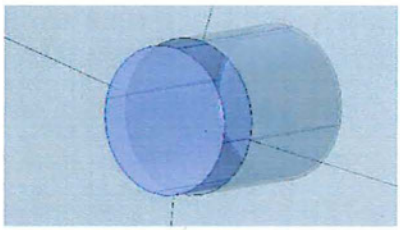

Figure 7.2: Cylindrical shape cut out of the sphere to create a proper boundary between the electrode and the solution inside the sphere.

After finishing the geometry, the physics concepts could be added. This research required the electric currents and the charged particle tracing module. The electrodes had a potential of $2.5\ V$ and $-2.5\ V$ to generate a dipolar electric field as shown in figure 7.3. The electric field points away from the positive electrode (left) and toward the negative electrode (right).

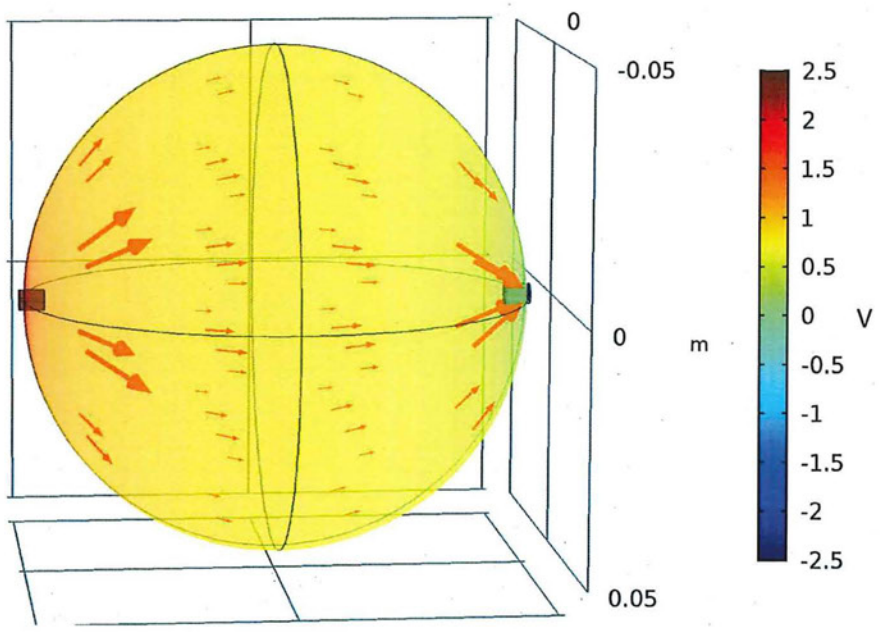

Figure 7.3: Electric field (arrows) created by two copper electrodes inserted into a sphere filled with a $2.8\ g/l$ $CuSO_4$ solution. The electrodes are at a voltage of $2.5\ V$ and $-2.5\ V$ as indicated by the color legend.

For the particle tracing, an inlet was added to each the bases of the cut out cylinders pointing into the center of the sphere. The inlet on the positive electrode released Cu^{2+} ions, while the inlet on the negative electrode released SO_4^{2-} ions. The Cu^{2+} ions had a mass of $m(Cu^{2+}) = 1.055 \times 10^{-25} kg$ and a charge of $q(Cu^{2+}) = 3.204 \times 10^{-1}\ C$. The SO_4^{2-} ions had a mass of $m(SO_4{}^{2-}) = 1.595 \times 10^{-25}\ kg$ and a charge of $q(SO_4{}^{2-}) = -3.204 \times 10^{-19}\ C$.

The particle trajectories were simulated for each inlet individually under only the electric force produced by the electrodes. Figure 7.4 shows the Cu^{2+} ion trajectories (left) and the SO_4^{2-} ion trajectories (right).

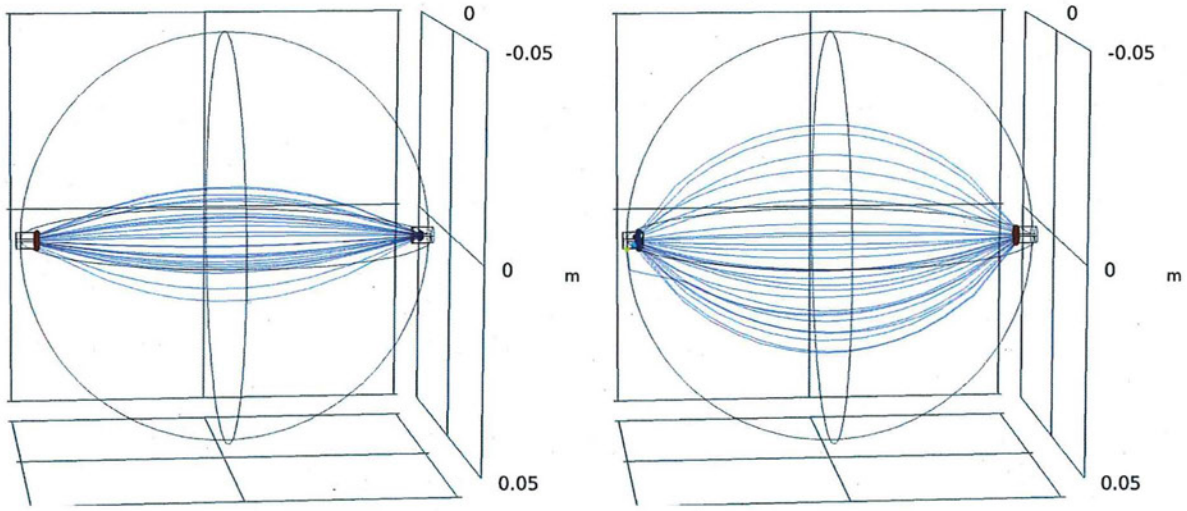

Figure 7.4: Simulated trajectories of Cu^{2+} and SO_4^{2-} ions subject to the electric field produced by two electrodes with voltages of 2.5 V (left electrode) and $-2.5\ V$ (right electrode).

Next, the constant magnetic field was added to simulate the magnetic field of an MRI scanner. A field of 4 T was applied in the positive z-direction perpendicular to the central axis of the electrodes. Figure 7.5 below shows the simulation results including the magnetic field. The ion trajectory now does not follow the electric field lines, as an additional magnetic force acts on the particles, which is described by equation 4.4 (Lorentz force equation).

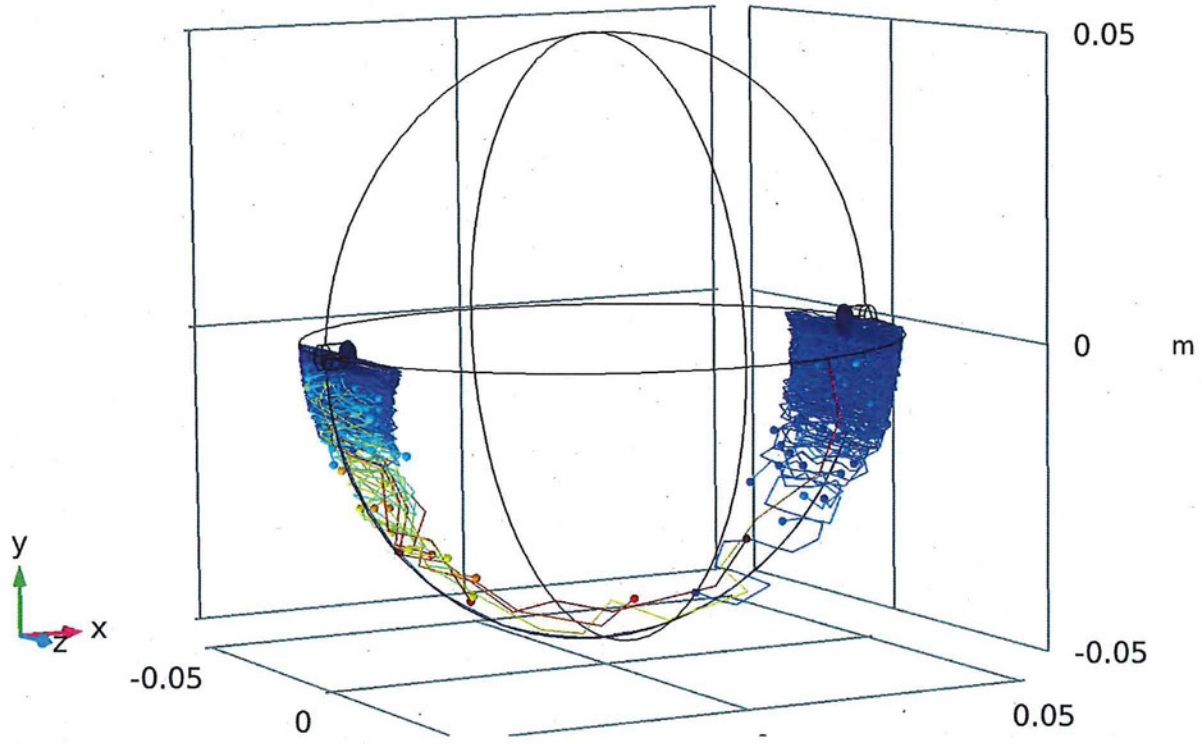

Figure 7.5: Simulated trajectories of Cu^{2+} and SO_4^{2-} ions subject to the electric field produced by two electrodes with voltages of 2.5 V (left electrode) and -2.5 V (right electrode) and to a magnetic field of 4 T in the positive z-direction.

These trajectories do not look like the ones predicted in [23], so simulation parameters were changed to achieve movement that more closely resembles the simulations in Truong, Avram, and Song's article. The magnetic field was changed to 0.1 T, which changed the ion paths to closer resemble the expected paths. This simulation result is shown in figure 7.6.

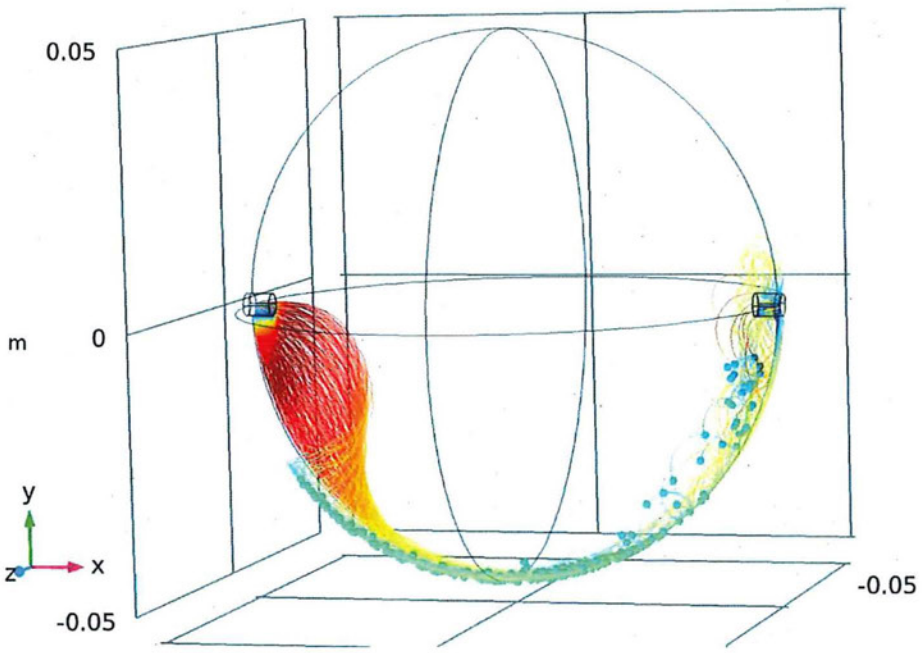

Figure 7.6: Simulated trajectories of Cu^{2+} and SO_4^{2-} ions subject to the electric field produced by two electrodes with voltages of 2.5 V (left electrode) and -2.5 V (right electrode) and to a magnetic field of 0.1 T in the positive z-direction.

The Cu^{2+} ions move in a circular path away from the positive electrode. The SO_4^{2-} ion trajectories, however, do not form a smooth circular path, but rather bounce along the walls of the sphere. Under closer examination in figure 7.7, the ions first move toward the positive x-direction, which is contrary to the expected movement in the negative x-direction due to the electric field.

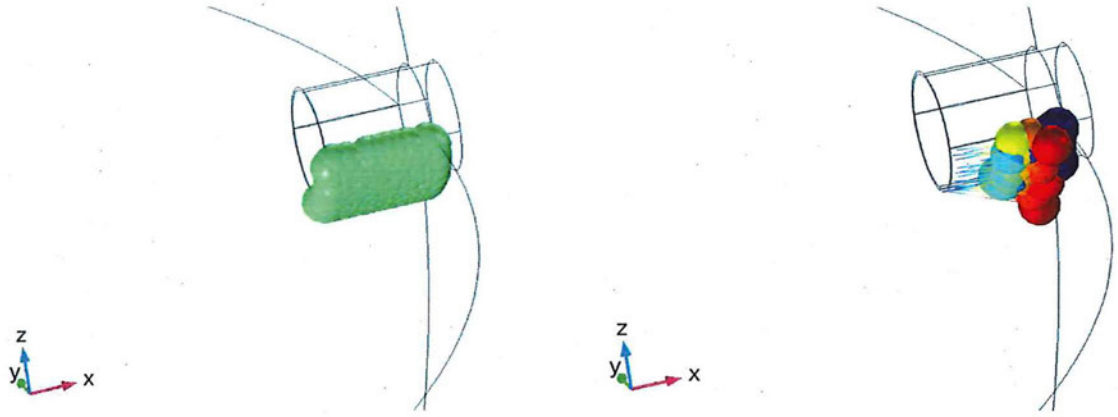

Figure 7.7: Close view of SO_4^{2-} ions subject to the electric field produced by two electrodes with voltages of 2.5 V (left electrode) and -2.5 V (right electrode) and to a magnetic field of 0.1 T in the positive z-direction. The left image shows the initial and the right image shows the final position. The ions are expected to move in the negative x-direction, not the positive x-direction.

8 Analysis and Discussion

Figure 7.3 shows the electric field produced by the two electrodes, whose direction and magnitude are as expected. The field points away from the positive electrode and toward the negative electrode. Its magnitude decreases, with increasing distance from the electrodes, as indicated by the size of the arrows. The ions in figure 7.4 follow trajectories that are expected from the electric part of the Lorentz force in equation 4.4. The positive Cu^{2+} ions move away from the positive electrode, while the negative SO_4^{2-} ions move toward the positive electrode. Due to their lower mass, the SO_4^{2-} ions experience a greater acceleration, which causes the radius of curvature of their trajectories to be larger than the radius of the Cu^{2+} ions' trajectories.

In figure 7.5, the ions are affected by the magnetic field more than the ones calculated by Truong, Avram, and Song in figure 6.1. The magnetic force on the ions is large, which causes the radius of curvature to be small, which in turn causes the ions to recoil from the walls of the sphere. In the simulation, no drag force due to collisions between ions and water molecules was specifically added. It was assumed that by defining material properties, the software would automatically add appropriate forces associated with the ion movement. This did not seem to be the case, which made the results in this thesis different than the ones obtained by Truong, Avram, and Song and corrected by Wijesinghe and Roth [23, 28]. Adding a drag force would decrease the velocity of the ions, and thus decrease the magnitude of the Lorentz force due to the magnetic field. This may cause the ions' trajectories to be close to what is expected.

To compensate for the lack of drag force, the magnetic field strength was decreased, which resulted in a smaller Lorentz force and a smoother circular movement shown in figure 7.6. The SO_4^{2-} ions, however, do not behave as expected. They move in a direction opposite to the electric force, before reflecting from the sphere wall. Even after switching the voltages of the electrodes and the particle inputs, the ions initially at this electrode always moved opposite to the force. I concluded that there was a glitch in the COMSOL software package that caused the unexpected movement.

The purpose of this thesis was not only to simulate ion movement, but also to experiment with COMSOL Multiphysics. This software has only been used by three other students at Ball State and is still in development. An important part of this thesis was to investigate whether this software could be used to simulate ion trajectories in a solution. Even though the desired results could not be successfully replicated, the possibilities and limitations of the software could be explored, and with changes to the model, the correct trajectories may be achieved.

References

[1] P.A. Bandettini, N. Petridou, and J. Bodurka. Direct detection of neuronal activity with MRI: fantasy, possibility, reality? *Applied Magnetic Resonance,* 26:65-88, 2005.

[2] P.A. Bandettini, E.C. Wong, R.S. Hinks, R.S. Tikofsky, and J.S. Hyde. Time course EPI of human brain function during task activation. *Magnetic Resonance in Medicine,* 25:390-397, 1992.

[3] J. Bodurka and P.A. Bandettini. Toward direct mapping of neuronal activity: MRI detection of ultraweak, transient magnetic field changes. *Magnetic Resonance in Medicine,* 47:1052-1058, 2002.

[4] A.M. Cassara, G.E. Hagberg, M. Bianciardi, M. Migliore, and B. Maraviglia. Realistic simulations of neuronal activity: A contribution to the debate on direct detection of neuronal currents by MRI. *NeuroImage,* 39:87-106, 2008.

[5] J.M. van Egeraat, R.N. Friedman, and J.P. Wikswo. Magnetic field of a single muscle fiber: First measurement and a core conductor model. *Biophysics Journal,* 57:663-667, 1990.

[6] J.M. van Egeraat and J.P. Wikswo. A model for axonal propagation incorporating both radial and axial ionic transport. *Biophysics Journal,* 64:1287-1298, 1993.

[7] S.J. Galioto, P.B. Reddy, A.M. El-Refaie, and J.P. Alexander. Effect of Magnet Types on Performance of High-Speed Spoke Interior-Permanent-Magnet Machines Designed for Traction Applications. *IEEE Transactions on Industry Applications,* 51 (3):2148-2160, 2015.

[8] A.A. Ghirardi. *Radio Physics Course*. Rienhart Books, New York, 1933.

[9] F.L.H. Gielen, R.N. Friedman, and J.P. Wikswo. In vivo magnetic and electric recordings from nerve bundles and single motor units in mammalian skeletal muscle. *Journal of General Physiology,* 98:1043-1061, 1991.

[10] F.L.H. Gielen, B.J. Roth, and J.P. Wikswo. Capabilities of a toroid-amplifier system for magnetic measurements of current in biological tissue. *IEEE Transactions on Biomedical Engineering,* 33:910-921, 1986.

[11] D.J. Griffiths. *Introduction to Electrodynamics*. Cambridge University Press, Cambridge, 2018.

[12] D.J. Griffiths. *Introduction to Elementary Particles*. Wiley-VCH Verlag, Weinheim, 2014.

[13] R.K. Hobbie and B.J. Roth. *Intermediate Physics for Medicine and Biology*. Springer, New York, 2011.

[14] S.A. Huettel, A.W. Song, and G. McCarthy. *Functional Magnetic Resonance Imaging*. Sinauer Associates, Sunderland, MA, 2014.

[15] D. Konn, P. Gowald, and R. Bowtell. MRI detection of weak magnetic fields due to an extended current dipole in a conduction sphere: A model for direct detection of neuronal currents in the brain. *Magnetic Resonance in Medicine,* 50:40-49, 2003.

[16] R.H. Kraus, P. Volegov, A. Matlachov, and M. Espy. Toward direct neural current imaging by resonant mechanisms at ultra-low field. *NeuroImage,* 39:310-317, 2008.

[17] T.S. Park and S.Y. Lee. Effects of neuronal magnetic field on MRI: Numerical analysis with axon and dendrite models. *NeuroImage,* 35::531-538, 2007.

[18] B.J. Roth and J.P. Wikswo. The magnetic field of a single nerve axon: A comparison of theory and experiment. *Biophysics Journal,* 48:93-109, 1985.

[19] R.A. Serway and J.W. Jewett. *Physics for Scientists and Engineers with Modern Physics*. Cengage, Boston, MA, 2014.

[20] E.P. Solomon, L.R. Berg, and D.W. Martin. *Biology.* Brooks and Cole, Belmont, CA, 2005.

[21] A.W. Song, A.M. Takahashi. Lorentz effect imaging. *Magnetic Resonance Imaging,* 19:763–767, 2001.

[22] K.R. Swinney and J.P. Wikswo. A calculation of the magnetic field of a nerve action potential. *Biophysics Journal,* 32:179-737, 1980.

[23] T.K. Truong, A. Avram, A.W. Song. Lorentz effect imaging of ionic currents in solution. *Journal of Magnetic Resonance,* 191:93-99. 2008.

[24] T.K. Truong, A.W. Song. Finding neuroelectric activity under magnetic-field oscillations (NAMO) with magnetic resonance imaging in vivo. *Proceedings of the National Academy of Science USA*. 103:12598–12601, 2006.

[25] T.K. Truong, J.L. Wilbur, A.W. Song. Synchronized detection of minute electrical currents with MRI using Lorentz effect imaging. *Journal of Magnetic Resonance*, 179:85–91, 2006.

[26] A. Webb. *Introduction to Biomedical Imaging*. Wiley, Hoboken, New Jersey, 2003.

[27] R.S. Wijesinghe and B.J. Roth. A model for compound action potentials and currents in a nerve bundle III: A comparison of the conduction velocity distributions calculated from compound action currents and potentials. *Annals of Biomedical Engineering,* 18:97-121, 1991.

[28] R.S. Wijesinghe and B.J. Roth. Lorentz effect imaging of ionic currents in solution using correct values for ion mobility. *Journal of Magnetic Resonance,* 204:225-227, 2010.

[29] J.P. Wikswo, J.P. Barach, and J.A. Freeman. Magnetic field of a nerve impulse: First measurements. *Science,* 208:53-55, 1980.

[30] J.P. Wikswo and J.M. van Egeraat. Cellular magnetic fields: Fundamental and applied measurements on nerve axons, peripheral nerve bundles, and skeletal muscle. *Journal of Clinical Neurophysiology,* 8:170-188, 1991.

[31] J.P. Wikswo, W.P. Henry, R.N. Friedman, W.A. Kilroy, R.S. Wijesinghe, J.M. van Egeraat, and M.A. Milek. *Intraoperative recording of the magnetic field of a human nerve.* Plenum, New York, 1990.

[32] J.K. Woosley, B.J. Roth, and J.P. Wikswo, The magnetic field of a single axon: A volume conductor model. *Mathematical Biosciences,* 76:1-36, 1985.

[33] X. Xue, X. Chen, T. Grabowski, and J. Xiong. Direct MRI mapping of neuronal activity evoked by electrical stimulation of the median nerve at the right wrist. *Magnetic Resonance in Medicine,* 61:1073-1082, 2009.

[34] H.D. Young and R.A. Freedman. *University Physics with Modern Physics*. Pearson Addison Wesley, San Francisco, 2008.

Appendix

Future students could pick up on this project and try to create a working model that includes a drag force on the ions. I have already started to work on a new model but have not completed enough of it to create working simulations. The new model includes the particle tracing for fluid flow module. Particle trajectories can be observed when applying a constant electric field, but when the electric field of the electrodes is used instead, the ions do not move at all. I hope that students interested in this research area can use this thesis as a guide for creating an improved model that includes all the parameters presented in [23] and [28] to more accurately simulate ion trajectories in solutions and advance technology to image neuronal activity using magnetic resonance imaging.

I want to describe possible ways to achieve the expected results as a guide for students interested in continuing this project. As mentioned above, I would advise switching from the charged particle trajectory module to the particle tracing for fluid flow module. In the latter, a drag force can be added that takes fluid viscosities into account. Another module that may be useful is the fluid-particle-interaction module, which could be used for more accurate boundary conditions. It also adds a multiphysics branch that considers interactions between particles and fluids and may make the simulations accurate. With these changes I hope that the results presented in articles [23] and [28] can be replicated using the correct parameters and progress can be made in this field of medical physics.